Int. J. Heat Mass Transfer. Vol. 23, pp. 413–424
Pergamon Press Ltd. 1980. Printed in Great Britain

BOUNDARY LAYER TRANSITION OBSERVATIONS ON A BODY OF REVOLUTION WITH SURFACE HEATING AND COOLING IN WATER

VIJAY H. ARAKERI
Mechanical Engineering Department, Indian Institute of Science, Bangalore 560012, India

(*Received* 1 *August* 1978 *and in revised form* 20 *February* 1979)

Abstract – Boundary layer flow visualization in water with surface heat transfer was carried out on a body of revolution which had the predicted possibility of laminar separation under isothermal conditions. Flow visualization was by in-line holographic technique. Boundary layer stabilization, including elimination of laminar separation, was observed to take place on surface heating. Conversely, boundary layer destabilization was observed on surface cooling. These findings are consistent with the theoretical predictions of Wazzan *et al.* in The stability and transition of heated and cooled incompressible laminar boundary layers, in *Proceedings of the Fourth International Heat Transfer Conference*, Vol. 2, FCI 4. Elsevier, Amsterdam (1970).

NOMENCLATURE

- D, maximum diameter of the test body;
- h, convective heat transfer coefficient;
- $\bar{h}$, average convective heat transfer coefficient from $(X/D)=0$ to $(X/D)=0.5$;
- K_f, thermal conductivity of water at T_f;
- K_m, thermal conductivity of copper;
- K_w, thermal conductivity of water at surface temperature;
- m, pressure gradient parameter, $(x/U_e)\mathrm{d}U_e/\mathrm{d}x$;
- Nu_D, Nusselt number, hD/K_w;
- $\overline{Nu}_D$, average Nusselt number, $\bar{h}D/K_f$;
- Re_D, Reynolds number, $U_\infty D/\nu$;
- r, local radius of the axisymmetric body;
- T_f, mean temperature, $(T_\infty+T_s)/2$;
- T_H, initial temperature of the heating water;
- T_s, local surface temperature;
- T_t, temperature indicated by the thermocouple;
- T_∞, free stream tunnel water temperature;
- ΔT, surface temperature difference, T_s-T_∞;
- t, wall thickness;
- U_e, local x-component velocity at the edge of the boundary layer;
- U_∞, free stream velocity;
- X, coordinate along the axis;
- x, coordinate along the surface.

Greek symbols

- α_r, wave number, $2\pi/\lambda_r$;
- β, Falkner–Skan parameter, $2m/(m+1)$;
- λ, Thwaites parameter $(\theta^2/\nu)\mathrm{d}U_e/\mathrm{d}x$;
- λ_r, disturbance wavelength;
- ν, kinematic viscosity of water at T_f;
- θ, boundary layer momentum thickness.

1. INTRODUCTION

WAZZAN *et al.* [1] have presented numerical calculations which show that laminar boundary layers in water can be stabilized by surface heating and destabilized by surface cooling. However, very few experimental investigations have been carried out which actually demonstrate the stabilization in the presence of finite levels of free stream turbulence, body vibrations, and noise. Some earlier efforts [2] have, in fact, been unsuccessful in showing the now predicted stabilization by surface heating. However, a recent study by Strazisar *et al.* (3) demonstrated the predicted stabilization on a flat plate.

If the predicted effects due to surface heat transfer are shown to exist under real situations, then practical applications may be forthcoming. Some of these applications are noted below:

(a) Reduction of drag by prolonging laminar flow by surface heating.
(b) Control of transition location by heating or cooling.
(c) Elimination of laminar separation by heating.

The first application is a well-known one with the anticipated reduction in the power, for example, to propel a body. The next two applications are mentioned on the basis of recent findings [4] that the existence of laminar separation and the location of transition itself can play significant roles in the inception and development of cavitation. Thus, improved model testing may be possible with the use of cooling to destabilize the boundary layer or use of heating to eliminate laminar separation which normally is not present for prototype conditions.

With some of these applications in mind, an axisymmetric body was chosen for the present experimental study. It had the predicted possibility of laminar separation under isothermal conditions but at the same time it did not possess extremely steep pressure gradients such that the viscous flow would be completely dominated by laminar separation. From previous experience [5], the proper body to select was a

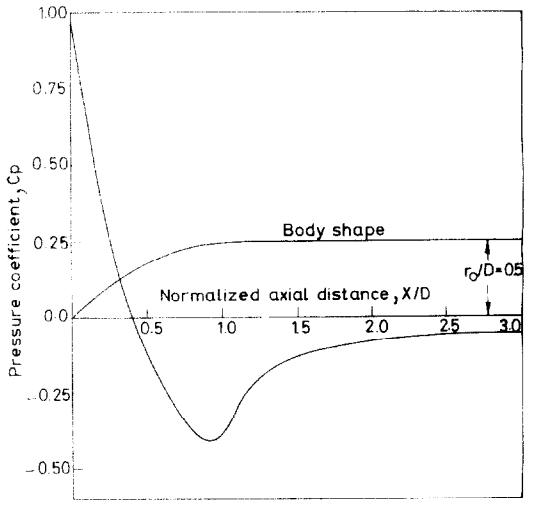

FIG. 1. Theoretical pressure distribution and the body shape for the 1.5 caliber ogive. Note the tangent point is located at $(X/D) = 1.118$.

1.5 caliber ogive with a cylindrical afterbody. The body shape and the theoretical pressure distribution* for the 1.5 caliber ogive are shown in Fig. 1. The boundary layer calculations described in the Appendix and presented in Fig. 2 show that Thwaites parameter reaches a maximum negative value of about 0.14 (normal criterion for separation is -0.09) for the 1.5 caliber ogive and then starts to decrease again. This shows that under isothermal conditions the likelihood of laminar separation is present, and the turbulent transition process will be expected to be influenced by its existence. Therefore, the boundary layer growth characteristics on a 1.5 caliber ogive are ideally suited for investigating the possibility of elimination of laminar separation by surface heating and its effects on the turbulent transition process. We might note here that in the experiments to be described, the Froude number will be of the order of 60 and therefore, buoyancy effects are not expected to play a role in the turbulent transition process with heat transfer.

In this paper, first the experimental methods used in the present study are described; then the results are presented and this is followed by a discussion of results. Subsequently, a section is devoted to interpreting the results of the present findings in the context of possible practical applications of surface heat transfer as a means of controlling the location of turbulent transition. Finally, a summary is provided.

2. EXPERIMENTAL METHODS

2.1. *Test facility*

The test facility used was the High Speed Water Tunnel at the Netherlands Ship Model Basin. Van der Meulen [6] has recently made use of this facility for flow visualization; since no modifications were required for the present experiments, details of the facility such as geometry of the test section etc. may be obtained from the above reference. The nominal maximum speed obtainable in a rectangular test section (50 mm × 50 mm) with rounded corners is about 30 m s^{-1}. Thus, for a body diameter of 10 mm, the maximum possible Re_D (Reynolds number based on maximum body diameter, free stream velocity, and kinematic viscosity at free stream temperature) is about 3×10^5 with room temperature water (20°C). However, by increasing the tunnel water temperature to 35°C, a maximum Re_D of the order of 4.5×10^5 could be attained. Operation of the tunnel at water

* The author would like to thank J. Carroll and Professor J. W. Holl of the Pennsylvania State University for these computations.

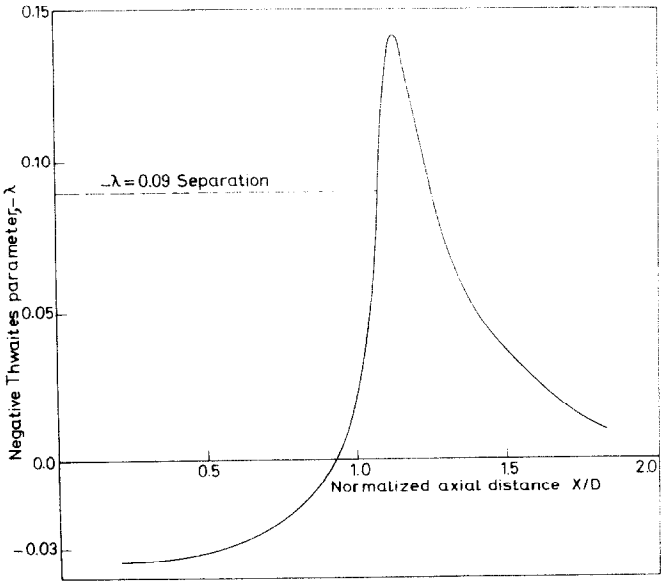

FIG. 2. Boundary layer Thwaites parameter vs normalized axial distance for the 1.5 caliber ogive.

temperatures significantly above 35°C proved to be unsafe.

2.2. *Test model*

The test model used for the present study was a 1.5 caliber radius tangent ogive with a cylindrical afterbody 10 mm in diameter. The model occupied 3.25% of the through flow area. This blockage was taken into account in the theoretical pressure-distribution calculations and the boundary layer growth computations shown in Figs. 1 and 2. For good heat transfer characteristics, the forward portion of the model was made of pure copper and the wall thickness was kept to a minimum possible value of 1 mm. The afterbody, attached to the nose by strong bonding epoxy adhesive, was made of stainless steel. Some details of the test body are noted in Fig. 3. The complete test body was securely attached to two struts which were mounted in the diffuser section of the tunnel.

The body was made by Instrumentum T.N.O. in Delft with extreme care. Inspection at a magnification of 20× proved that the model contour was within 5 μm of the theoretical shape. In addition, the nominal surface roughness was quoted to be of the order of 0.6 μm.

2.3. *Heating and cooling*

Surface heating or cooling was achieved by internal circulation of hot or cold water within the forward portion of the test body. The circulating water was finally ejected from the test body into the tunnel water. General flow direction of the circulating water is noted in Fig. 3. This technique proved to be a simple and effective means of surface heating or cooling. However, since the tunnel water had a capacity of about 60 l., only limited quantities of heating or cooling water could be circulated at a time without altering tunnel operating conditions. The heating and cooling water was stored in a cylindrical ($D = 7.3$ cm) container of about 1.25 l. capacity. Circulation was started and maintained by pressurizing the water free surface in the container to 2 atm above the tunnel working pressure. This typically provided a flow rate of 0.05 l. s^{-1}, and an approximately 25 s period of steady internal water circulation. It was found from the model wall temperature measurements that essentially steady state conditions were achieved within about half the period of steady internal water circulation.

2.4. *Temperature measurements*

A single iron–constantan thermocouple was embedded in the nose of the test body to measure the wall temperature. Details of the mounting of the thermocouple are shown in Fig. 4. The thermocouple* used was only sensitive at the tip, and the relatively small size (1.0 mm diameter) provided an excellent time response. A second thermocouple was placed in a constant temperature water bath whose temperature was measured accurately to within 0.1°C with a mercury thermometer. The differential reading from the two thermocouples was amplified so that the final sensitivity was 10 mv/°C. The amplified reading was measured with a digital voltmeter which could be read to an accuracy of 0.1 mv. Thus, under steady state conditions it was possible to read the model temperature to an accuracy of 0.1°C. However, under the quasi-steady state conditions of the present experiments, the accuracy of the measured model tempera-

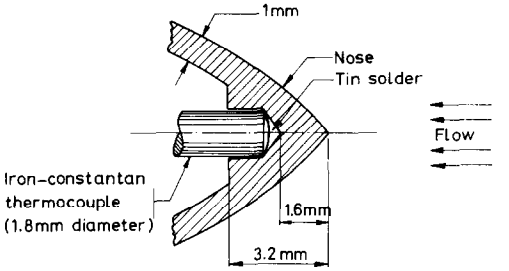

FIG. 4. Details of thermocouple mounting in the nose.

* Thermocoax, S. A. Sodern, France.

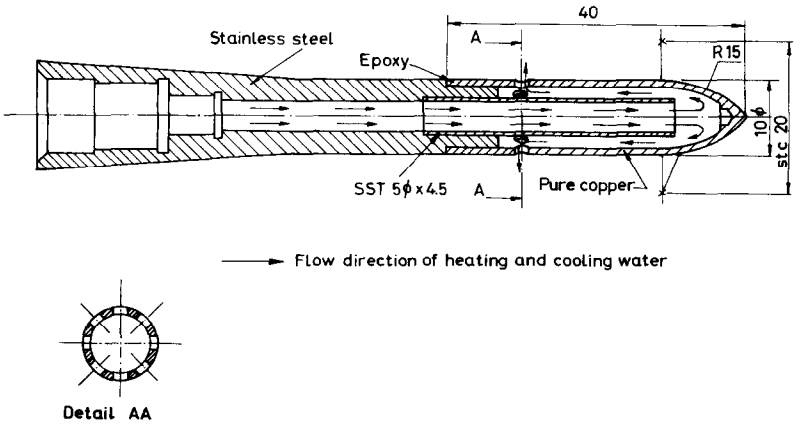

FIG. 3. Geometrical details of the test body (dimensions in mm).

ture can be claimed to be within 0.5°C. The tunnel water temperature could be measured with the same thermocouple mounted in the nose of the model. This reading was obtained without any internal circulation of hot or cold water.

Due to the thinness of the wall and the extremely good thermal conductivity of copper, it was expected that the thermocouple in the nose would be sensitive to heat transfer rates from the forward portion of the model and not only to heat transfer rates confined to the immediate nose area. This was confirmed by a calibration run with the nose of the model insulated by a thin coating (few microns) of plastic paint up to an axial distance of $(X/D) = 0.35$. This insulation did not affect the wall temperature reading, supporting our above conjecture. In view of this, so that the surface temperature could be inferred, the temperature readings from the thermocouple were corrected by estimating the average heat transfer coefficient up to $(X/D) = 0.5$ following the methods outlined in reference [7] (see Appendix for details). The maximum correction at a Re_D of 1.8×10^5 was of the order of 6°C. The estimated surface temperature distribution as shown in Fig. 12 of the Appendix illustrates that the surface temperature is reasonably constant downstream of $(X/D) = 0.44$ and that the correction procedure for inferring the surface temperature from the thermocouple readings is quite adequate.

2.5. *Flow visualization*

Flow visualization in the present work was done by making in-line holograms of the flow field covering a region of $(X/D) = 0$ to $(X/D) = 2.5$ of the test body. A schematic diagram of the optical set-up used in making the holograms is shown in Fig. 5. The essential details of the present technique of flow visualization may be found in [6]. Briefly, a pulsed ruby laser with an exposure time of 25 ns was used as a light source. To improve the resolution of the system, the red light from the ruby laser was converted to ultraviolet light with a wavelength of 0.347 μm. The holograms were recorded on Agfa 8E56 plates.

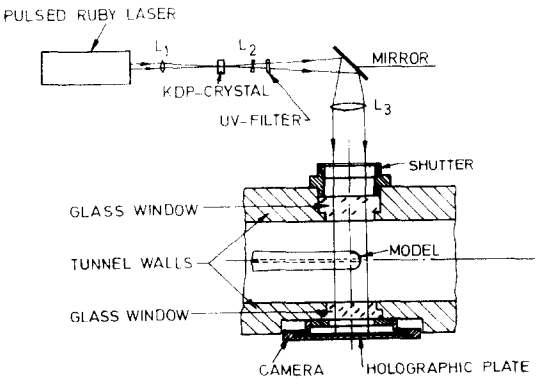

FIG. 5. Schematic diagram of the optical set-up for making the in-line holograms (Courtesy of Dr. J. H. J. Van der Muelen).

In the case of heating, the thermal boundary layer deflects the light away from the model and the hologram records the interference of this deflected light with the undeflected light which acts as the reference wave. During reconstruction with a helium–neon laser the interference causes a real image not only of the body but also of the thermal boundary layer. This real image could then be studied in detail with a microscope with magnifications up to 200. Normal magnification used in the present work was 28 × or 40 ×. This is one of the principle advantages of holographic flow visualization.

In the case of cooling, the thermal boundary layer deflects the light into the model so it then cannot interfere with the reference wave which is blocked by the model. Thus, the cooled situation could not be studied in the reconstruction set-up. In any case, it should be noted here that for both the heated and cooled cases the holographic recording is also the normal shadowgraph recording. Thus, cases of cooling could still be studied in the shadowgraph sense but not in the holographic sense. The shadowgraph images in these cooled cases were analysed at a magnification of ten.

2.6. *General experimental procedure*

The normal experimental procedure was first to fix the tunnel temperature either by complete cooling, limited cooling, or no cooling of the tunnel water. In the latter cases frictional heat increased the tunnel water temperature. Thus, when the desired tunnel water temperature (constantly monitored by the thermocouple in the nose) was reached, the test velocity was adjusted. Then the heating or cooling water was supplied to the container and its temperature was noted. At the same time, the power supply for the ruby laser was charged. Just prior to activating the switch to initiate circulation of the hot or cold water, the tunnel temperature was noted. Once the ruby laser was ready to be fired, the solenoid valve was activated and started the circulation of the hot or cold water. Initially the wall temperature changed rapidly; however, within about 10 s the change was quite slow being of the order of $0.1°C\,s^{-1}$. After about 20 s of water circulation the hologram was recorded and the model temperature was noted down. After two to three runs the injected water was bled out of the tunnel. Nominal test Reynolds numbers, Re_D, were 7×10^4, 1.2×10^5, 1.8×10^5, and 2.4×10^5. A few recordings were made at higher Reynolds numbers. For cooling, normal tunnel water temperatures were 20°C and 35°C, and initial cooling water temperatures were of the order of 2°C, 10°C, and 15°C. For heating, normal tunnel water temperature was 17–20°C, and initial heating water temperatures were of the order of 35°C, 50°C, 65°C, and 80°C.

3. EXPERIMENTAL RESULTS

3.1. *Separation under isothermal conditions*

As shown in Fig. 2, the 1.5 caliber ogive is predicted

to possess laminar separation under isothermal or no heat transfer conditions. For the present method of flow visualization, a certain amount of heating of the surface was required. It was noticed that with surface temperature differences of the order of 2–3°C, boundary layer separation could not be clearly detected. However, with temperature differences of the order of 5–6°C, boundary layer separation could clearly be observed. Since lesser amounts of heating should promote separation and not suppress it [1], it can be concluded that under isothermal conditions the 1.5 caliber ogive does possess laminar separation as predicted. An example exhibiting separation and detail of the separated region are shown in Fig. 6. The average location of separation was found to be $(X/D) = 1.095$, and the predicted location is $(X/D) = 1.065$.

3.2. *Separation with surface heating*

With a temperature difference between the model surface and the free stream of 12°C or larger, laminar separation could no longer be detected on the 1.5 caliber ogive. With a temperature difference of less than 12°C, the separation streamline could be clearly reconstructed as shown in Fig. 6. However, with a temperature difference of the order of 12°C or slightly more, the separation streamline could not be clearly reconstructed and instead a fringe pattern appeared in the expected region of laminar separation (see Fig. 7). With a temperature difference greater than 15–16°C, even the fringe pattern disappeared and an attached boundary layer could be reconstructed in the region and downstream of the expected location of laminar separation.

3.3. *Transition under isothermal conditions*

Since test Reynolds numbers in the present experiments were below the predicted critical Reynolds number of 6.28×10^5 [5] for the 1.5 caliber ogive, the transition process was taking place on the separated streamline. However, as shown in the photograph of Fig. 6, the separated streamline is extremely close to the model surface and thus, the stability characteristics may be close to those for the separating velocity profile ($\beta = -0.1988$). As was the case for separation, transition could clearly be seen in the present experiments only with surface temperature differences of the order of 5°C or higher. Typically, the laminar portion could be seen to become unstable in the sense of spatial waviness, and at a short distance downstream the thermal boundary layer could not be visualized further presumably due to mixing of temperature gradients. The point of disappearance of the thermal boundary layer was taken to indicate the transition to turbulence. The variation of this with Reynolds number in the present experiments is shown in Fig. 9. Also shown are results from earlier observations [5] of transition by the schlieren technique on a 50 mm 1.5 caliber ogive. It may be noted that the present results agree well with those found on the larger body at the California Institute of Technology.

3.4. *Transition with surface heating*

The movement of the transition location with increased surface heating is shown in the photographs of Fig. 8. In presenting these photographs, significant details have been lost; however, as noted earlier the details could be studied in the reconstruction set-up. Typically, amplified boundary layer waves could be observed within the attached boundary layer (with temperature difference greater than 12°C). The waves would persist for some distance in the downstream direction and would eventually break up, clearly indicating a turbulent boundary layer. Some of these details are apparent in the photographs of Fig. 7. Thus, one could identify the instability location where the distortion in the boundary layer could first be observed and one could also identify the transition location where the wave would break up and the turbulent boundary layer could be observed. The measured axial distances, to instability and transition locations with increased surface heating are shown in Fig. 10 for a Reynolds number of 1.8×10^5.

Using the reconstruction set-up, it was possible in addition to measure the wavelength of the amplified disturbances in the boundary layer. These measurements were restricted to (X/D) values of 1.325–1.5, where the average negative Thwaites parameter is about 0.05. However, in studying the holograms it was clear that the initial amplification of the disturbances was taking place even upstream of a (X/D) value of 1.325, where the negative Thwaites parameter values are close to the separation value of 0.09. In view of this, it was felt that it would be justifiable to compare the present measurements with theoretical predictions [1] for separating velocity profiles. Additional comments on this point will be made in Section 4. In any case, the present measurements with a Reynolds number based on a momentum thickness of 350 at $(X/D) = 1.325$ are shown in Fig. 11 along with theoretical predictions. We might note here that the use of momentum thickness is preferred since it changes little with increasing surface temperature, compared to the displacement thickness [1]. Thus, only a small error is introduced in using the value of momentum thickness calculated on the basis of isothermal conditions even with heat transfer. In particular, this is the case for the maximum temperature differences encountered in the present experiments.

3.5. *Transition with surface cooling*

As noted previously, cases of cooling could only be studied by the shadowgraph technique. The existence of laminar separation was indicated but could not be clearly observed. However, surface cooling should promote separation and not suppress it [1]. Thus, it can be concluded that laminar separation on surface cooling was occurring. Instability and transition location as defined earlier could be visualized quite clearly by the shadowgraph technique. Typical photographs of the cooled cases made from the original

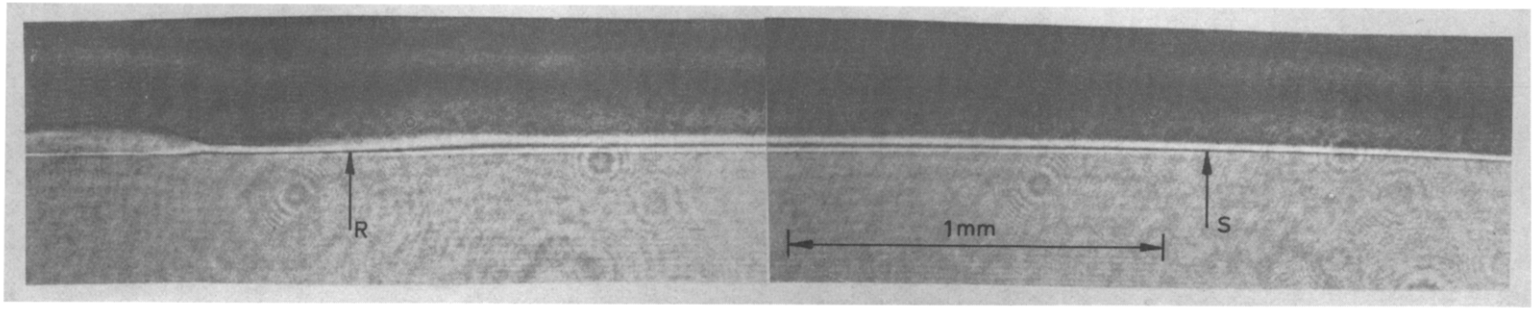

FIG. 6. Photograph showing details of laminar separation (S) and reattachment (R) on a 1.5 caliber ogive. (X/D) at separation is 1.102. The flow is from right to left. $\Delta T = +5°C$, $Re_D = 1.8 \times 10^5$.

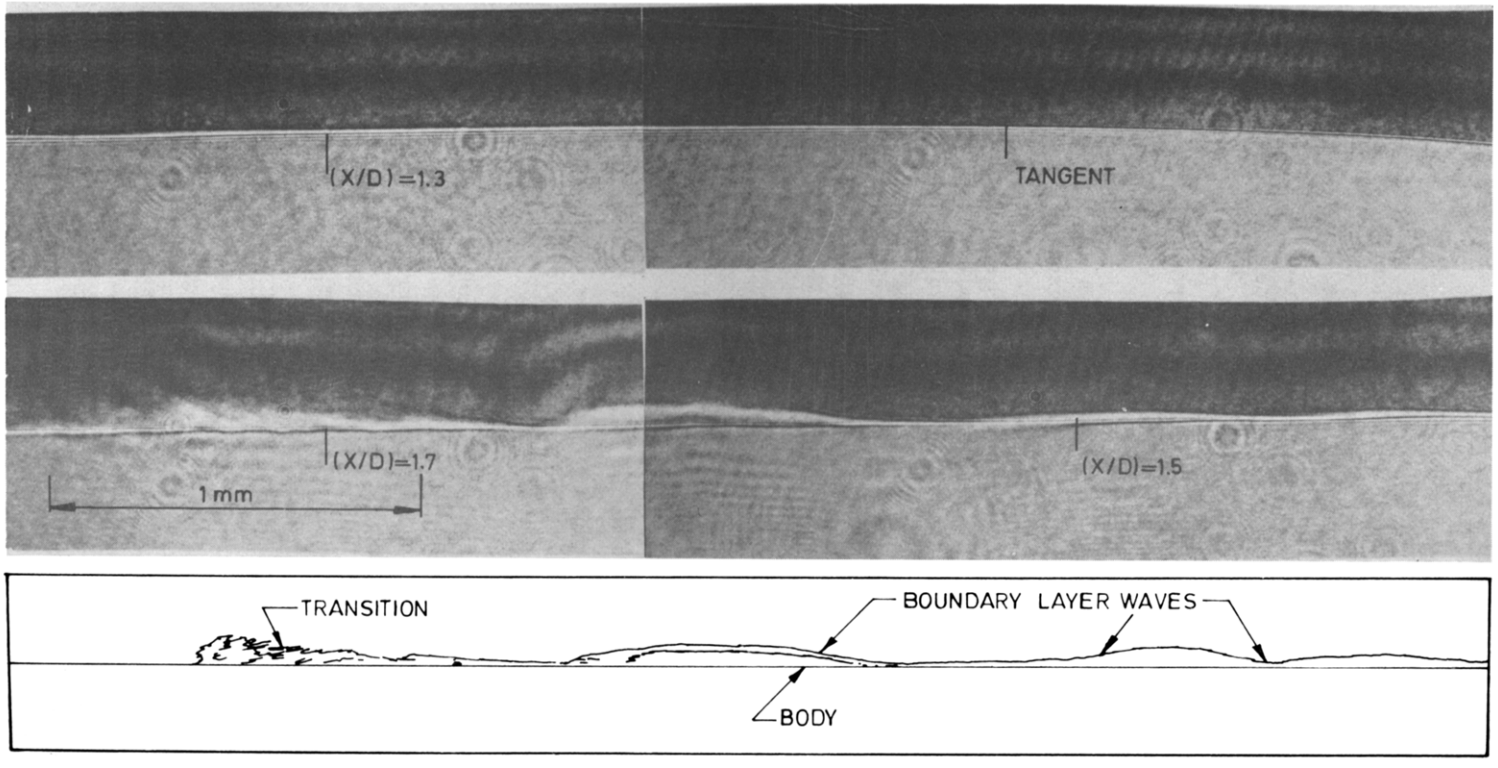

FIG. 7. Photograph showing details of transition process on a 1.5 caliber ogive. The flow is from right to left. Note separation is eliminated. $\Delta T = +12°C$, $Re_D = 1.8 \times 10^5$.

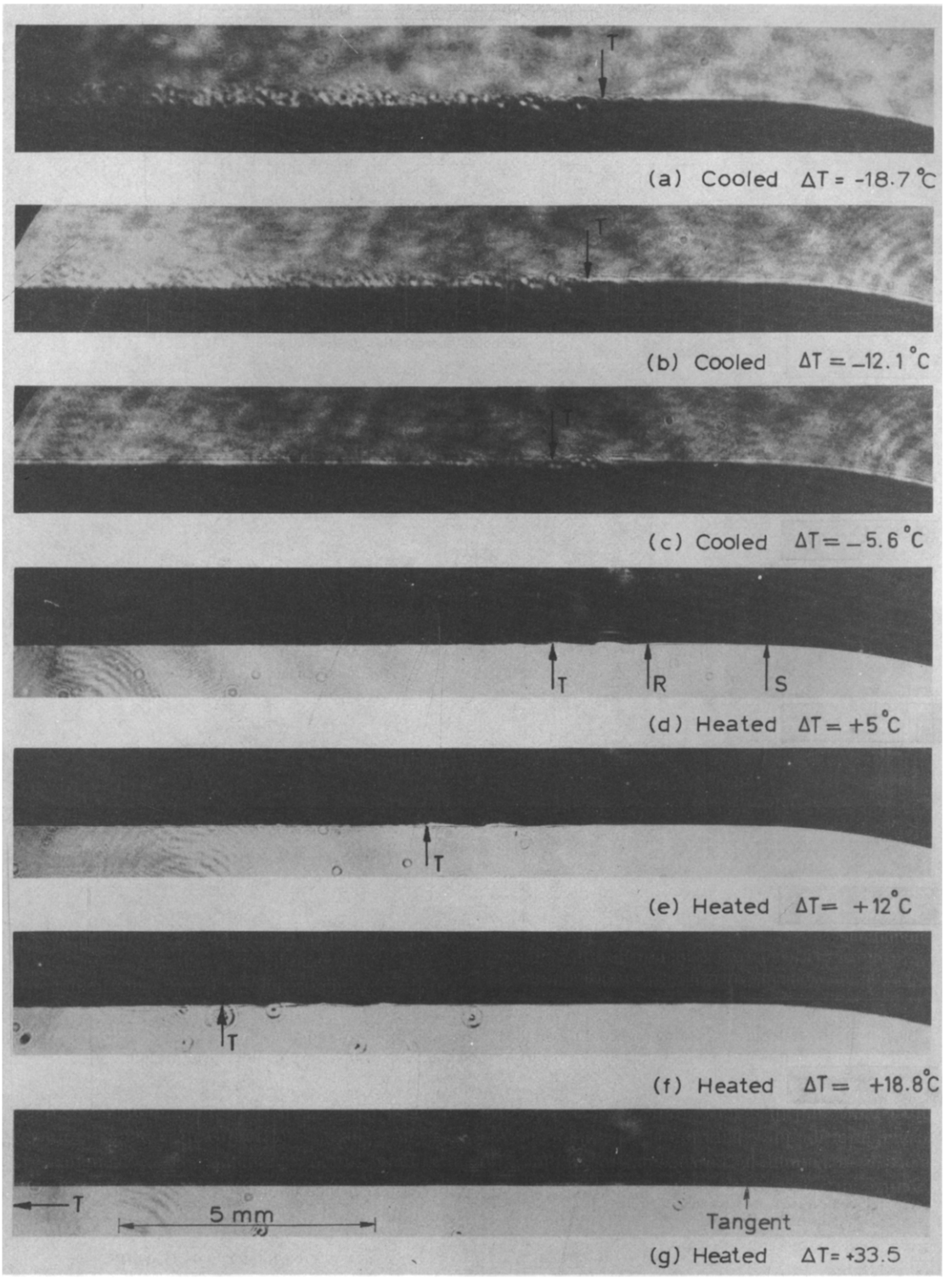

FIG. 8. Boundary layer transition (T) with surface heating and cooling. Cooled cases from shadowgraph and heated cases from reconstruction set-up. The flow is from right to left. $Re_D = 1.8 \times 10^5$. S is separation and R reattachment.

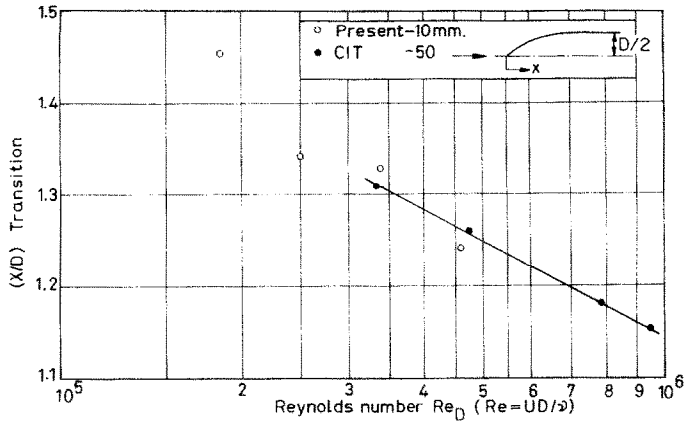

FIG. 9. Location of transition vs Reynolds number under isothermal conditions (slight heating). Present observations on a 10 mm body with in-line holography. Previous observations on a 50 mm body with schlieren technique.

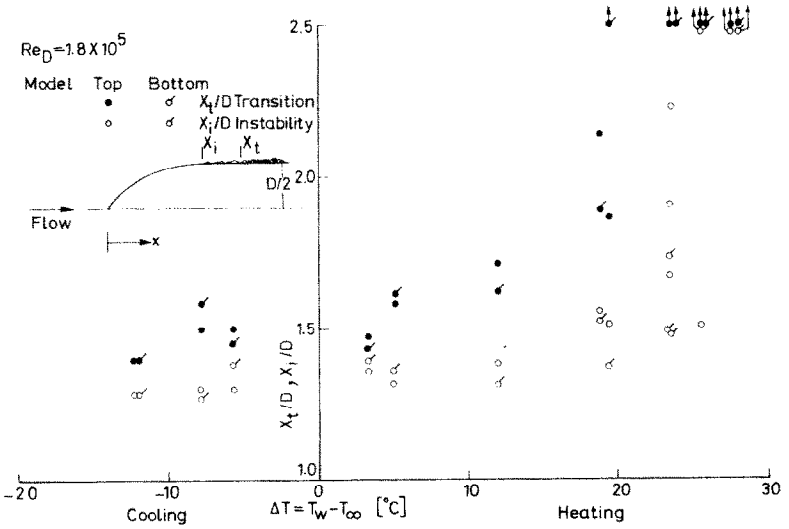

FIG. 10. Influence of heating and cooling on the location of instability and transition on a 1.5 caliber ogive. Points with arrows indicate locations beyond the view of holographic flow visualization.

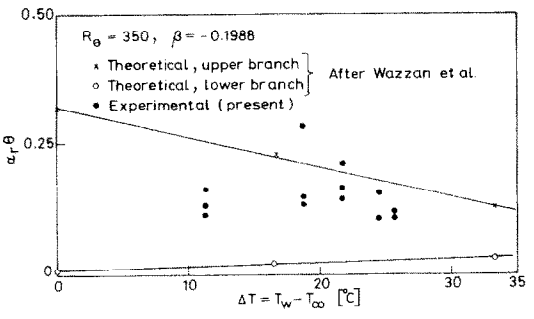

FIG. 11. Comparison of measured wavelength of amplified disturbances with theoretical predictions in the presence of surface heating. ($\alpha_r = 2\pi/\lambda_r$, θ is boundary layer momentum thickness, and λ_r is wavelength of the disturbance).

hologram are shown in Fig. 8. The measured axial distances to instability and transition locations with increased surface cooling are shown in Fig. 10 for a Reynolds number of 1.8×10^5.

4. DISCUSSION OF RESULTS

Present observations of boundary layer transition under isothermal conditions (slight heating) agrees very well with previous observations on a larger body at the California Institute of Technology (C.I.T.) water tunnel facility (Fig. 9). From this we might infer that the free stream turbulence level in the present facility is of the same order as that in the C.I.T. facility which has been measured to be about 0.2%.

From the results presented in Figs. 6 and 7 it is clear

that surface heating can eliminate laminar separation as predicted by computations [1]. For the 1.5 caliber ogive, the minimum value of Thwaites parameter is −0.141 as shown in Fig. 2. Thus, by surface heating to 12°C above the free stream temperature, the separation criterion based on Thwaites parameter was increased to −0.141, i.e. an increase of 56.5% from the normal criterion of −0.09. This provides a quantitative estimate for the prediction of the elimination of laminar separation by surface heating. From simplified theoretical estimates [8] an increase of 56.6% in the Falkner–Skan pressure gradient parameter from the normal value of −0.1988 for separation would require a wall overheat of 62.5°C. Thus, the simplified theoretical predictions clearly underestimate the effectiveness of surface heating in the elimination of laminar separation.

The boundary layer stabilization by surface heating is also evident from the photographs of Fig. 8 and from the results presented in Fig. 10. At a Re_D of 1.8×10^5, the point of instability is hardly influenced by surface heating up to about 12°C even though the location of transition does shift downstream. It may be recalled that separation is first eliminated for this level of heating. For higher levels of heating when laminar separation is eliminated, the location of both instability and transition move downstream. However, with surface heating of about 27.5°C above the free stream temperature, the character of the laminar boundary layer essentially changes. Within the holographic field of view of $(X/D) = 2.5$, no disturbances could be detected even at magnifications of 200×. Thus, within the resolution of the holographic technique of flow visualization, complete stabilization up to $(X/D) = 2.5$ was achieved at the critical temperature difference of 27.5°C. A rough comparison of this observed critical temperature difference with the theoretical computations of Wazzan *et al.* [1] can be made. From boundary layer calculations the Reynolds number based on momentum thickness* at the location of laminar separation is about 200 and the corresponding critical temperature difference required for stability is 40°C based on the computations of Wazzan *et al.* In the present experiments the critical temperature difference for stability was found to be 27.5°C. Thus, the level of heating required to stabilize the boundary layer is found experimentally to be less than predicted by theory. However, the theory is for neutral stability whereas in the experiments the observed stability may not in fact correspond to neutral stability due to limited resolution. What is observed in experiments is most likely the significantly reduced amplification of disturbances resulting from surface heating. In any case the trend noted in the present experiments certainly is in complete agreement with theoretical predictions. This is further supported by the results presented in Fig. 11. The observed wave numbers of the amplified disturbances mainly fall within the restricted zone predicted by theory [1]. The results discussed so far are mostly for Re_D of 1.8×10^5. At other Reynolds numbers, stabilization with surface heating was observed. For example, at a Re_D of 7×10^4, a stable free shear layer was observed to exist up to $(X/D) = 2.5$ with surface heating of 10°C above the free stream temperature. However, at a Re_D of 2.4×10^5, complete stability could not be achieved due to the restricted capability of surface heating. The transition location did move downstream to $(X/D) = 1.92$ with a surface temperature difference of 25.5°C compared to the transition location of $(X/D) = 1.35$ observed with slight heating.

For the cooled situation, the point of instability and the location of transition did move upstream with increased cooling (Figs. 8 and 10). Thus, the boundary layer was destabilized by surface cooling, which is consistent with the predictions of Wazzan *et al.* [1]. We might note here that for the cooled cases, boundary layer transition was taking place along the separated free shear layer.

Finally, it must be emphasized here that the favourable comparisons noted between the experimental observations of the present work and the theoretical predictions of Wazzen *et al.* [1] can be claimed to be only qualitative. The principle reason for this being the fact that the boundary layer growth on the present test body is non-similar, (meaning that the Thwaites parameter or equivalently the Falkner–Skan β parameter varies continuously with spatial coordinates), whereas, the theoretical computations are for similar growth with β remaining constant. Recently, it has been clearly pointed out by Wazzan and Gazley [9] that for axisymmetric bodies of the type used in the present experiments the boundary layer 'history' can have an important effect on the stability characteristics and local conditions may be appreciably different from wedge flow having the same Falkner–Skan parameter.

5. DESIGN IMPLICATIONS

It is clear from the present findings that the location of turbulent transition can be controlled by surface heating or cooling. In addition, elimination of laminar separation by surface heating is also possible. However, there are certain observations from the present study which have implications in estimating the heat transfer requirements, or more appropriately the level of surface heating, necessary to stabilize the boundary layer on a body of revolution. Typically, in the downstream direction the negative value of Thwaites parameter (equivalently the Falkner–Skan parameter) will vary for a body of revolution as shown in Fig. 2 with peak values in the neighbourhood of the tangent point. In some cases the peak values may exceed the separation criterion as was the case for the 1.5 caliber ogive. In any case, the region near the peak values will be the 'critical zone' from the stability point of view. On the 1.5 caliber ogive at a Re_D of 1.8×10^5 transition

* Again the use of momentum thickness over displacement thickness is preferred since the latter changes significantly with surface heating whereas the former does not.

was observed to occur near $(X/D) = 1.75$ with surface heating of 19°C. It should be noted that near $(X/D) = 1.75$, the values of Thwaites parameter are around -0.01 or close to that for a flat plate case. Therefore, on the basis of flat plate stability considerations for surface heating of 19°C, the boundary layer should have been completely stabilized [1], and this perhaps would be the case with steady boundary layer growth. However, in the presence of boundary layer disturbances which were amplified in the critical zone, stability characteristics have been altered significantly. It is pertinent to point out that in some cases the maximum height of the boundary layer waves observed in the present experiments was greater than the height of the separated free shear layer under conditions of slight heating. Thus, estimates of heating requirements for sustained boundary layer stabilization should pay special attention to the stability characteristics in the critical zone. For the 1.5 caliber ogive, complete stabilization in the critical zone was required for sustained stabilization downstream. This apparently means that there will be an upper bound on Re_D for sustained stabilization limited by the stability characteristics of the critical zone. For example, the upper bound for the 1.5 caliber ogive is about five million based on the stability characteristics of the separating profile [1].

6. SUMMARY

Existing laminar boundary layer separation on a body of revolution was eliminated by surface heating to a temperature difference of 12°C. Such a body possesses a maximum value for Thwaites parameter of -0.141. The normal criterion for separation is -0.09. Thus, quantitatively, the normal Thwaites criterion is increased by 56.6% when the surface temperature is 12°C higher than the free stream temperature. In the present work, boundary layer flow visualization was by in-line holographic technique. Transition observations by the same technique under isothermal conditions (with slight heating) are in good agreement with previous observations in the California Institute of Technology water tunnel facility on a larger body. Transition observations under surface heated conditions clearly showed the predicted stabilization at all the test Reynolds numbers. At a Re_D of 1.8×10^5 with surface heating to a temperature difference of 27.5°C, no disturbances in the laminar boundary layer could be observed with magnification of 200×, up to the limit of the holographic view at $(X/D) = 2.5$. Under isothermal conditions at the same Re_D, transition is observed at $(X/D) = 1.45$. With cooling, transition did move upstream indicating destabilization. Thus, the present observation of boundary layer stability in the region of laminar separation and downstream are entirely consistent with the theoretical predictions of Wazzan *et al.* [1].

Acknowledgements – The work reported here was carried out at the Netherlands Ship Model Basin during the author's stay there as a Visiting Scientist. The author would like to thank Professor J. D. Van Manan, Drs. M. W. C. Oosterveld and J. H. J. Van der Muelen for making his stay at NSMB possible. The author is particularly grateful to Dr. D. H. J. Van der Muelen for his assistance in conducting the experiments. The work was sponsored by Ministerie Van Defensie (Marine), Bureau Scheepsbouw, Den Haag. The author is also grateful to Dr. Carl Gazley Jr. of the Rand Corporation for bringing to his attention and making available to him certain references quoted in the text and the Appendix.

REFERENCES

1. A. R. Wazzan, T. T. Okamura and A. M. O. Smith, The stability and transition of heated and cooled incompressible laminar boundary layers, in *Proceedings of the Fourth International Heat Transfer Conference*, Vol. 2, Paris–Versailles FC1.4. Elsevier, Amsterdam (1970).
2. R. Siegel, the effect of heating on boundary layer transition for liquid flow in a tube, Ph.D. Thesis, Massachusetts Institute of Technology (1953).
3. A. J. Strazisar, E. Reshotko and J. M. Prahl, Experimental study of the stability of heated laminar boundary layers in water, *J. Fluid Mech.* **83,** 225–248 (1978).
4. V. H. Arakeri and A. J. Acosta, Viscous effects in the inception of cavitation on axisymmetric bodies, *J. Fluids Engng* **95,** 519–528 (1974).
5. V. H. Arakeri, A note on the transition observavations on an axisymmetric body and some related fluctuating wall pressure measurements, *J. Fluids Engng* **97,** 82–87 (1975).
6. J. H. J. Van der Muelen, A holographic study of cavitation on axisymmetric bodies and the influence of polymer additives, Ph.D. Thesis, Enschade, Holland (1976). (Also available as Netherlands Ship Model Basin Report.)
7. W. M. Kays, *Convective Heat and Mass Transfer*, pp. 222–226. McGraw-Hill, New York (1966).
8. J. Aroesty and S. A. Berger, Controlling the separation of laminar boundary layers in water: heating and cooling, Report No. R-1789-ARPA, The Rand Corporation, California (1975).
9. A. R. Wazzen and C. Gazley, Jr., The combined effects of pressure gradient and heating on the stability and transition of water boundary layers, in *Second International Conference on Drag Reduction, St. John's College, Cambridge, England*, pp. 23–40 (1977).
10. L. F. Crabtree *et al.*, Three dimensional boundary layers, in *Laminar Boundary Layers*, edited by L. Rosenhead, pp. 430–432. Oxford University Press, Oxford (1963).
11. V. H. Arakeri, Viscous effects in inception and development of cavitation on axisymmetric bodies, Ph.D. Thesis, California Institute of Technology, California (1973).
12. G. M. Harpole *et al.*, Approximate methods for calculating the properties of heated laminar boundary layers in water, Report No. R-2165-ARPA, The Rand Corporation, California (1978).
13. H. Martin, Impinging jet flow heat and mass transfer, in *Advances in Heat Transfer*, Vol. 13, pp. 10–15. Academic Press, New York (1977).
14. W. M. Kays, *Convective Heat and Mass Transfer*, pp. 175–180. McGraw-Hill, New York (1966).

APPENDIX

(a) *Laminar boundary layer growth calculations*

These were made using Thwaites' approximate method which is detailed for axisymmetric bodies in reference [10] (also see [11]–[13]). The method involves the computation of a parameter $\lambda = (\theta^2 U_e'/\nu)$ using the expression

$$\lambda = \frac{0.45}{r^2} \frac{U_e'}{U_e^6} \int_0^x r^2 U_e^5 \, dx,$$

where θ is the momentum thickness, U_e is the local velocity at

the edge of the boundary layer, U'_e is the local spatial derivative of U_e, and r is the local radius of the axisymmetric body. The integral was evaluated numerically using results of the potential flow calculations. The location of laminar separation is taken to be the point where λ has a value of -0.09. The author has previously [11] used this method and the criterion to predict laminar separation on several axisymmetric bodies—to predict laminar separation on several axisymmetric bodies. The predictions compared quite favourably (within 7%) with the measurements. We might note here that the present computations do take into account the blockage effects encountered in the present work; however, no attempt is made to include heat transfer effects on the boundary layer growth calculations.

(b) *Estimation of spatial surface temperature distribution*

The estimation which is valid in the region of laminar flow was carried out numerically by dividing the body [up to $(X/D) = 2.5$] into subdivisions. A heat flow balance was expressed for each subdivision in terms of the nodal temperatures, and the resulting simultaneous equations were solved numerically by relaxation method so that the accuracy of each nodal temperature was within ± 0.5°C. The Nusselt number, $Nu_D = hD/K_w$, for the outer surface was calculated by the method outlined in [7]. The method uses the wedge flow solutions, and to account for the viscosity variation with surface heating, the wedge flow solutions computed by Harpole *et al.* [12] were utilized for present computations. For an expected surface temperature difference of about 27°C, the estimated value of Nu_D near $(X/D) = 0$ was about 1300 and it decreased to about 250 at $(X/D) = 2.5$.

The Nusselt number for the inner surface exposed to the heating or cooling water was estimated by considering the forward portion, up to $(X/D) = 0.96$, to be heated by an impinging jet (with hydraulic diameter as the characteristic length), and the downstream portion to be heated by annular flow. The Nusselt number for impinging jet heating was obtained from [13], and for annular heating with the present geometry and Reynolds number by extrapolating results from [14]. The viscosity variation was taken into account by using the standard procedures suggested for turbulent flow in tubular geometry. It is expected that with the present annular geometry, entrance effects would be important; however, there was no available data which could be employed to make appropriate corrections. Instead, the Nu_D at $(X/D) = 0.96$ where the impinging jet heating is assumed to end was joined smoothly to the asymptotic value of Nu_D calculated for the fully developed flow in the annular geometry. Typically, the Nu_D was found to vary from 1000 to 500 in the jet heated portion, and from 500 to 170 in the annular heated portion.

The computed surface temperature distribution for one of the extreme cases of heating with $Re_D = 1.8 \times 10^5$, the temperature of the heating water equal to 80°C, and the temperature of the free stream equal to 17°C is shown in Fig. 12. It may be noted that up to $(X/D) = 0.44$, strong temperature gradients are predicted; however, subsequently the maximum deviation from the value at $(X/D) = 0.44$ is 1.5°C.

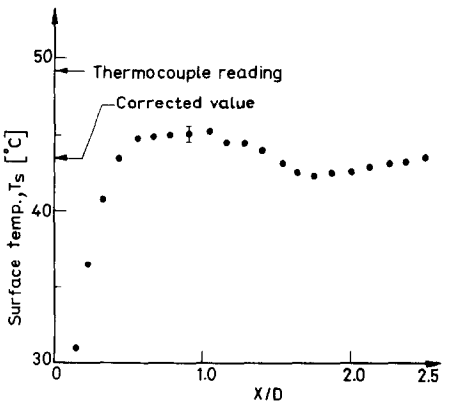

FIG. 12. Estimated dependence of surface temperature on normalized axial distance. $Re_D = 1.8 \times 10^5$, $T_\infty = 20$°C, and $T_H = 80$°C. Also noted are the thermocouple reading under these conditions and the inferred surface temperature as the corrected value.

(c) *Correction applied to infer surface temperature from thermocouple reading*

The correction was applied on the basis of heat balance which can be written down in non-dimensional form as follows:

$$\frac{T_t - T_s}{T_s - T_\infty} = \overline{Nu_D} \frac{K_f}{K_m} \frac{t}{D},$$

T_t is the temperature indicated by the thermocouple, T_s is the surface temperature, T_∞ is the free stream fluid temperature, $\overline{Nu_D}$ is the Nusselt number based on the average heat transfer coefficient from $(X/D) = 0$ to $(X/D) = 0.5$, K_f is the fluid thermal conductivity evaluated at the mean temperature $T_f = (T_s + T_\infty)/2$, K_m is copper thermal conductivity, t is the minimum distance from the centre point of the thermocouple to the surface (equal to 0.15 mm), and D is the maximum diameter (equal to 10 mm). The average heat transfer coefficient, $\bar{h}$, was evaluated following the procedures outlined in [7] using the isothermal wedge flow solutions. Quantitatively, the difference $(T_t - T_s)$ was found to be 5.7°C for one of the extreme cases of heating and is shown in Fig. 12. We might note that from the same figure that the corrected value seems to indicate the estimated surface temperature quite accurately downstream of $(X/D) = 0.44$. It may be pointed out here that the correction procedure was arrived at strictly from calibration runs, and the results of Fig. 12 were computed subsequently. It is clear though that mounting of additional thermocouples would have been highly desirable, however, this was not practically feasible due to the physically small size of the test body employed.

OBSERVATIONS SUR LA COUCHE LIMITE DE TRANSITION D'UN CORPS DE REVOLUTION DANS L'EAU AVEC CHAUFFAGE OU REFROIDISSEMENT DE LA SURFACE

Résumé — On visualise l'écoulement de couche limite dans l'eau à la surface d'un corps de révolution qui permet une séparation laminaire sous des conditions isothermes. La visualisation utilise la technique holographique en ligne. On observe la stabilisation de la couche limite, avec suppression de la séparation laminaire sur une surface chauffée et au contraire une déstabilisation sur une surface refroidie. Ces faits sont compatibles avec les prévisions théoriques de Wazzan *et al.* dans "La stabilité et la transition d'une couche limite laminaire chauffée et refroidie", *Proceedings of the Fourth International Heat Transfer Conference, Vol.* 2, FC1.4. Elsevier, Amsterdam (1970).

BEOBACHTUNGEN DES GRENZSCHICHTVERHALTENS AN EINEM VON WASSER UMSTRÖMTEN ROTATIONSSYMMETRISCHEN KÖRPER MIT BEHEIZTER BZW. GEKÜHLTER OBERFLÄCHE

Zusammenfassung— An einem rotationssymmetrischen Körper, an dessen Oberfläche Wärme an strömendes Wasser übertragen wird, wurde die Grenzschichtströmung mittels Holografie sichtbar gemacht. Am Körper war unter isothermen Bedingungen rechnerisch die Möglichkeit der laminaren Ablösung zu erwarten. Wenn die Oberfläche beheizt wurde, konnte Stabilisierung der Grenzschicht bis zur Vermeidung der laminaren Ablösung beobachtet werden. Umgekehrt wurde festgestellt, daß bei Kühlung der Oberfläche die Grenzschicht instabil wurde. Diese Ergebnisse stimmen überein mit den theoretischen Vorhersagen von Wazzan *u. a.* in der Veröffentlichung "The stability and transition of heated and cooled incompressible laminar boundary layer", *Proceedings of the Fourth International Heat Transfer Conference*, Vol. 2, FCI 4. Elsevier, Amsterdam (1970).

ИССЛЕДОВАНИЕ ПЕРЕХОДА ПОГРАНИЧНОГО СЛОЯ НА ТЕЛЕ ВРАЩЕНИЯ ПРИ НАГРЕВАНИИ И ОХЛАЖДЕНИИ ПОВЕРХНОСТИ В ВОДЕ

Аннотация — Визуализация течения в пограничном слое в воде при наличии теплообмена на поверхности проводилась на теле вращения, на котором в изотермических условиях возможен ламинарный отрыв потока. Визуализация осуществлялась с помощью голографического устройства. При нагревании поверхности наблюдалась стабилизация пограничного слоя и отсутствие отрыва. И наоборот, при охлаждении поверхности наблюдалась дестабилизация пограничного слоя. Эти результаты согласуются с теоретическими результатами, полученными Ваззаном и др. в работе «Устойчивость и переход нагретого и охлажденного несжимаемого ламинарного пограничного слоя», опубликованной в томе 2 Трудов 4-ой международной конференции по теплообмену (1970 г.).